The multi-phase nature of three intracluster media

Massimiliano Bonamente [1], and Richard Lieu [1]

[1]Department of Physics, University of Alabama, Huntsville, AL 35899, U.S.A.

Received _____; accepted _____

arXiv:astro-ph/0001128v1 8 Jan 2000

ABSTRACT

Among the models proposed to account for the new component of diffuse EUV and soft X-ray emission from clusters of galaxies (first discovered in Virgo [1]) are two key contestants: the non-thermal scenario which postulates a population of relativistic electrons undergoing inverse-Compton (IC) interaction with the cosmic microwave background [2,3], and the original conjecture [1] that the radiation is from a thermal warm gas at a temperature of $\sim 10^{5-6}$ K. Currently a consensus set of limiting values on cosmological parameters favor the thermal gas interpretation [4]. We also argued, based on pressure balance within the intracluster medium (ICM), that the non-thermal approach has formidable difficulties [5]. Here we describe a spatial analysis of the soft X-ray excess emission of three clusters (Virgo, A2199, and Coma), using archival ROSAT/PSPC data, which reveals resolved features of cold intracluster clouds in absorption spreading over vast distances. Within the sample there is good indication that the soft excess radial trend (SERT, which qualitatively means a rising importance of the soft component with cluster radius) is due to a centrally peaked distribution of cold matter, with Coma having the least effect and no direct evidence for absorption. The data strongly suggest an intermixed ICM which contains gas masses at a wide range of temperatures, and the soft excess is due to a warm intermediate phase.

In an accompanying work we found several pieces of evidence, based mainly on the detection of cloud silhouettes in the EUV, that the ICM of the cluster A2199 is multi-phase [5]. This *Letter* presents X-ray (0.2 - 2.0 keV) data, taken by the PSPC, of a cluster sample which provide independent results pointing to a generally intermixed ICM with important roles played by gas phases at temperatures lower than that of the hot (virial) gas.

We begin with Virgo, and show in Figure 1 the SERT in the 1/4 keV band with three noteworthy points. Firstly, the line-of-sight HI column density (N_H) was shown by a recent 21 cm measurement [1] to radially increase from $N_H = 1.8 \times 10^{20}$ cm^{-2} at the cluster center to $N_H = 2.0 \times 10^{20}$ cm^{-2} at the radius interval of 15 – 19 arcmin. This was confirmed by IRAS 100 μm images [6], consequently in Figure 1 we already took its effect on the SERT into account. Secondly, given the radial HI gradient (which continues its rising trend beyond 19 arcmin), and the known anti-correlation between HI and the 1/4 keV diffuse sky background [7], one must assess how much the PSPC background was underestimated when it was determined, as in our case, from a $\sim$ 40 – 50 arcmin annulus centered at M87. Of most concern are the 10 –15 and 15 – 19 arcmin annuli, where the 1/4 keV sky background accounts for 12 – 21% of the detected flux in this band. A re-scaling of this background in accordance with the HI gradient [7] over the corresponding regions only leads to a negligible effect on the 1/4 keV excess (viz. a reduction by 1 – 2% from our reported values of 30 – 40 % excess). Thirdly, a statistically significant rising SERT was also revealed by our recent EUVE (0.069 - 0.19 keV) observation of Virgo, which featured an *in situ* background measurement by means of the offset pointing technique detailed earlier [8]. It is however the higher signal-to-noise PSPC data which enable us to probe the nature of the soft emission using image diagnostics.

We provided facts which form a compelling case for interpreting the SERT as due, at least in part, to intracluster absorption by an even cooler phase [5]. This *Letter* explains why we are confronted with the reality of widespread absorption - the PSPC has already resolved the effect into small clouds distributed throughout the ICM. Such an inference was made after evaluating the smoothness of the 1/4 keV excess image (for details on the procedures used to obtain this image, see the caption of Figure 1). Specifically the presence or not of deviations in the spatial distribution of signals from Poisson behavior was assessed. As a control experiment, we initially applied the test to a 'blank field', acquired

during a PSPC pointed observation of the (undetected) UV star beta Leonis, when the field was not illuminated by any source other than the sky background. When this background was subtracted in the normal manner (i.e. using an outer field annulus to determine it, and correcting for vignetting effects before applying to another part of the detector) the resulting spread of significances follows, as expected, a gaussian of null mean value and σ= 1, see Figure 2.

The same method was then applied to three annuli of Virgo. The results, displayed in Figure 3, indicate the presence of spatial structures in Virgo's soft emission. The soft excess is clearly revealed by the positive mean value at all radii. However, even if the data are fitted with a σ=1 gaussian of variable mean, the agreement remains unsatisfactory, due to residuals at negative σ, which can only be interpreted as signatures of absorption at scale lengths $\leq$ the Point Spread Function (PSF) of the PSPC, where the soft component is silhouetted by cold clouds along the line-of-sight. Starting from the cluster center (0 – 4 arcmin from M87), we found on the $-\sigma$ side a deviation from the expected (best-fit) gaussian by $+\sim 11$ % in the total number of scanned regions. The effect decreases with radius, since the same percentage deviation reduces to $+\sim 4$ % in the 4 – 7 arcmin annulus, and further out there is no longer any evidence for non-gaussian behavior. This radially declining influence of absorption - an explanation of the SERT - is naturally understood in terms of a centrally condensed distribution of cold gas. In Figure 4 we show the three deepest absorption features which exist in the central area, positionally coincident with prominent radio lobes [9] and with locations where the hot ICM has a lower reported temperature [10].

We proceed to the next cluster of our sample, A2199, where again we focus on the PSPC image. At EUV energies a strongly rising SERT was found for this cluster [5]. Yet the same is not true in soft X-rays, as is shown in Figure 5 where it can be seen that while

the center exhibits flux depletion, analogous to the EUV, the outer radii are not associated with a soft excess, nor with a rising trend. Could absorption have played a role in this large scale radial behavior ? Our simulations indicate that that it is indeed possible to compare and contrast the EUV with the soft X-rays in terms of a warm component which has a large intrinsic EUV to soft X-ray flux ratio, coupled with Galactic *and* an appropriate amount of intracluster absorption (the latter with N_H between a few $\times$ 10^{19} and 10^{20} cm^{-2}) along the line-of-sight. The outcome is an absorbed flux which remains within the sensitivity of the EUVE observation, but evades detection by the PSPC.

Such a scenario is put to test by spatially analyzing the distribution of the soft excess of A2199, Figure 6. The central region corresponds to a gaussian of expected width but negative mean, symptomatic of a large absorption area wherein the clouds are unresolved [5]. As one moves towards the outer radii the best gaussian mean shifts towards *positive* values while the $\sigma = 1$ width does not fit the left half, where a 'tail' of resolved absorption clouds is evident. This 'tail' biases the data mean towards negative values, producing the illusion of an overall depletion in soft X-rays when there actually is an *excess* flux. The discovery of absorbing clouds then applies at least out to a radius of 10 arcmin ($\sim$ 0.4 Mpc for $H_o = 75$), implying an area $\sim$ 25 times larger than that of the cooling flow, and $\sim$ 3 times larger than that of the central EUV 'shadow' [5].

Equally revealing are the PSPC data of Coma, our last cluster, as it provides more independent scrutiny of the intermixed model. This cluster has a weak (i.e. nearly flat) SERT, although there is a soft X-ray excess at all radii [11], see Figure 7. According to our proposed interpretation, then, the ICM of Coma would probably not be as subject to absorption effects as the other clusters. This is confirmed by the spatial distribution of the soft excess, which shows no evidence for deviation from a smooth (i.e. gaussian) behavior in any annulus, Figure 8. The absence of a cooling flow in Coma may be the reason why

there is less cold gas, although such an explanation does not account for the detection of absorption in A2199 at radii of 7 – 10 arcmin. A more plausible idea is that the generation of a cold phase does not proceed at high rates when the hot ICM has an unusually high temperature, as is the case for Coma.

In conclusion, analysis of PSPC images of three clusters revealed that the two which exhibit a strong SERT (Virgo and A2199) also have a widespread distribution of absorbing clouds, rendering the prospect of interpreting the SERT as an absorption effect attractive. Typical values for the mass and column density of the cold gas, as estimated from the data, are respectively $\sim 5 \times 10^{10}$ $M_\odot$ Mpc^{-3} and $\sim$ a few $\times 10^{19}$ cm^{-2} [5]. The soft excess takes the form of a hitherto unresolved glow of diffuse emission filling the ICM, since (unlike absorption) there is no evidence in the PSPC images for isolated emission 'blobs'. Thus the possibility of a warm intermediate phase which has larger filling factor than the cold phase has also become attractive. Certainly one can no longer continue with the notion of the soft excess as a systematic effect of some kind [12,13]: if the gaussian means can be centered at zero (rather than their currently positive values) as a result of correcting such effects, one must face the absurdity of interpreting the 'tails' at negative σ as absorption of null signals.

References

1. Lieu, R., Mittaz, J.P.D., Bowyer, S., Lockman, F.J., Hwang, C. -Y., Schmitt, J.H.M.M. 1996a, *Astrophys. J.*, **458**, L5–7.
2. Hwang, C.-Y. 1997, *Science*, **278**, 1917.
3. Sarazin, C.L., Lieu, R. 1998, *Astrophys. J.*, **494**, L177–180.
4. Cen, R. and Ostriker, J.P. 1999, *ApJ*, **514**, 1-6.
5. Lieu, R., Bonamente, M. and Mittaz, J.P.D 2000, *Nature* submitted.
6. Wheelock et al. 1994, *IRAS Sky Survey Explanatory Supplement*, (JPL Publication 94-11), Pasadena, CA.
7. Snowden, S.L., Egger, R., Finkbeiner, D.P., Freyberg,M.J. and Plucinsky, P.P. 1998, *Astrophys. J.*,**493**, 715.
8. Lieu, R., Bonamente,M. ,Mittaz, J.P.D., Durret, F., Dos Santos, S. and Kaastra, J.S. 1999, *ApJ*, **527**, L77.
9. Harris, D.E., Owen, F., Biretta, J.A., and Junor, W. 1999, *Proceedings of the Workshop 'Diffuse thermal and relativistic plasma in galaxy cluster'*, Ringberg Castle Germany, MPE report 271, 111.
10. Boehringer, H. 1999 , *Proceedings of the Workshop 'Diffuse thermal and relativistic plasma in galaxy cluster*, Ringberg Castle Germany, MPE report 271, 115.
11. Lieu, R., Mittaz, J.P.D., Bowyer, S., Breen, J.O., Lockman, F.J., Murphy, E.M. and Hwang, C.-Y. 1996, *Science*, **274**, 1335.
12. Arabadjis, J.S. and Bregman, J.N. 1999, *Astrophys. J.*, **514**, 607.
13. Bowyer, S., Berghoefer, T.W and Korpela, E.J. 199, **Astrophys. J.**, **526**, 592.
14. Mewe, R., Gronenschild, E.H.B.M. and van den Oord, G.H.J. 1985, *A & A*, **62**, 197 .
15. Mewe, R., Lemen, J.R., and van den Oord, G.H.J. 1986, *A & A*, **65**, 511 .
16. Kaastra, J.S. 1992 in *An X-Ray Spectral Code for OpticallyThin Plasmas*

(Internal SRON-Leiden Report, updated version 2.0).

17. Kaastra, J.S., Lieu, R., Mittaz, J.P.D., Bleeker, J.A.M., Mewe, R., Colafrancesco, S. and Lockman, F.J. 1999, *Astrophys. J.*, **519**, L119.

Figure captions

Figure 1: The SERT effect of the Virgo cluster, illustrated by a plot against cluster radius of the soft X-ray fractional excess η, defined as $\eta = (p - q)/q$, where for a given annulus p is the observed 1/4 keV band (defined here as PSPC PI channels 18-41, or $\sim 0.2 - 0.4$ keV) flux after subtracting the sky background, and q is the expected flux from the hot ICM as determined by fitting the PI channels 50 – 200 ($\sim 0.5 - 2.0$ keV) using the MEKAL thin plasma emission code [14 - 16] and Galactic absorption as described in the text. Note that the same subtraction of background and hot ICM contribution was applied, except to individual regions rather than entire annuli, when we investigated the spatial distribution of the 1/4 keV band excess in Figures 2, 3, and 5.

Figure 2: A statistical test of the small scale smoothness of a typical PSPC 1/4 keV sky background in a 'blank field' observation, using a region of the detector ~ 20 arcmin off-axis. The 'background' was determined from another region ~ 40 arcmin off-axis, and was subtracted from the first region after vignetting correction. The spatial distribution of the resulting signals were sub-divided equally into small boxes of size 0.5 arcmin $\times$ 0.5 arcmin, and a histogram is plotted to show the number of occurences above and below a mean value of zero in units of σ, the standard deviation of each box obtained by adding in quadrature the respective Poisson errors in the measured flux and the subtracted component. The box size is larger than the PSPC PSF at all energies, and encloses sufficient counts to ensure that one is in the gaussian limit. The best-fit gaussian (dashed line) is obtained by varying only the mean, to accomodate the possibility of a finite (i.e. positive or negative)

subtracted signal: its width remains fixed at unit σ, while its normalization is determined by the conservation of total box number. The best mean is fully consistent with zero, and the absence of fit residuals implies that the test reveals smoothness of the image.

Figure 3: A statistical test of the small scale smoothness of the 1/4 keV excess in Virgo. The three regions of concern were divided into small boxes as described in Figure 2, the same applies to the best-fit gaussian.

Figure 4: The image of 1/4 keV excess of Virgo, expressed in units of σ above and below the null mean value expected for the case of no soft excess, where σ is defined in Figure 2 and the box size used for computations is 1.25 arcmin $\times$ 1.25 arcmin. The cross marks the position of M87. Pockets of absorption are evidently embedded in an unresolved glow of soft excess emission.

Figure 5: As in Figure 1, except now for the cluster A2199. The Galactic line-of-sight HI column density used is our measured value of 8.3×10^{19} cm^{-2} [17].

Figure 6: As in Figure 3, except now for the cluster A2199. See also the information given in Figure 5.

Figure 7: As in Figure 1, except now for the Coma cluster. The Galactic line-of-sight HI column density used is our measured value of 8.7×10^{19} cm^{-2} [11].

Figure 8: As in Figure 3, except now for the Coma cluster. See also the information given in Figure 7.

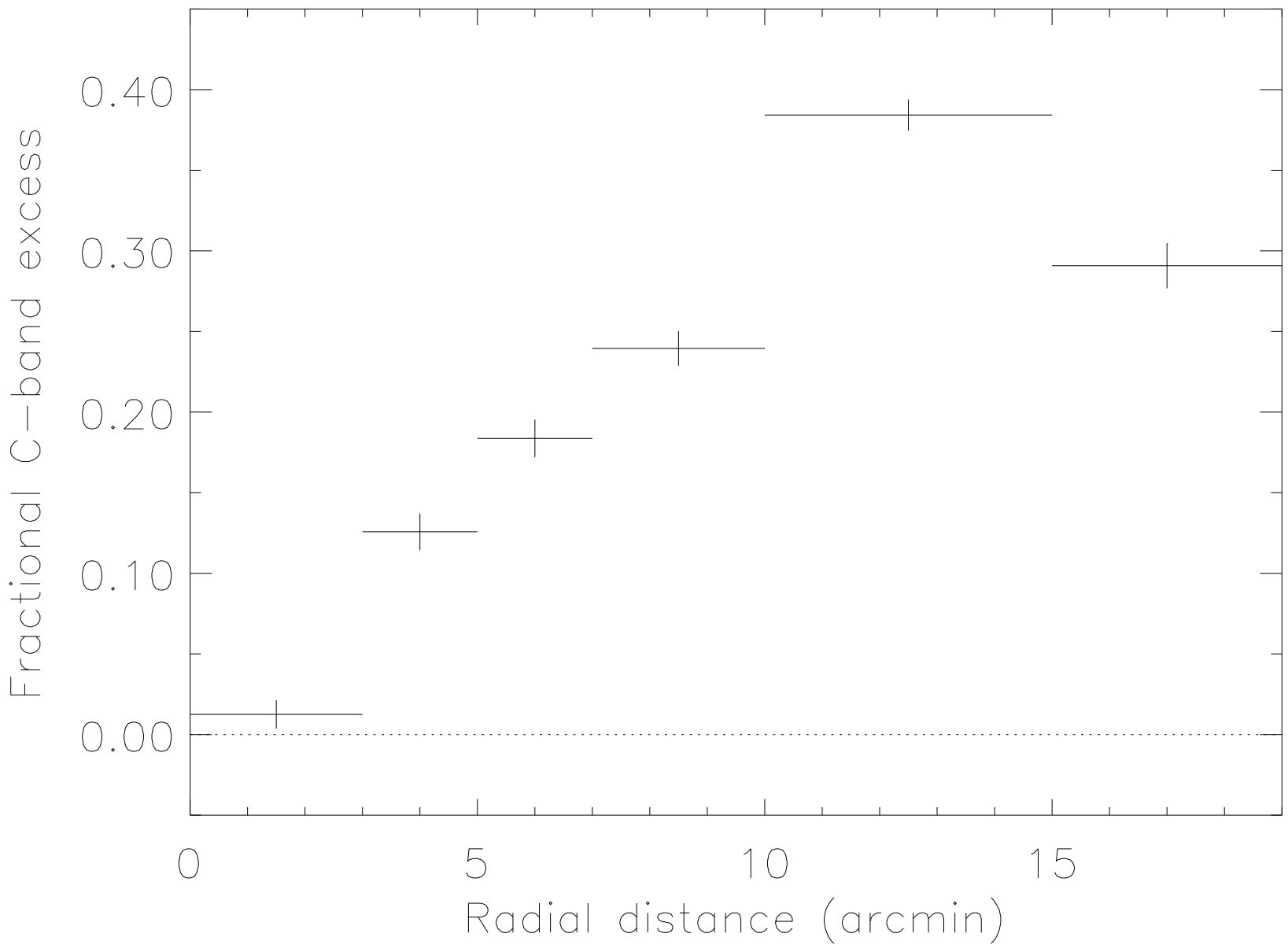
0.40
0.30
0.20
0.10
0.00
Fractional C-band excess
0
5
10
15
Radial distance (arcmin)

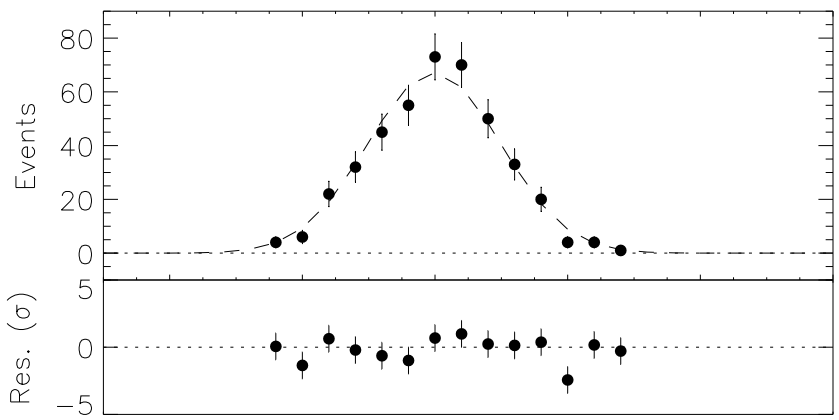
Events
80
60
40
20
0
Res. (σ)
5
0
−5

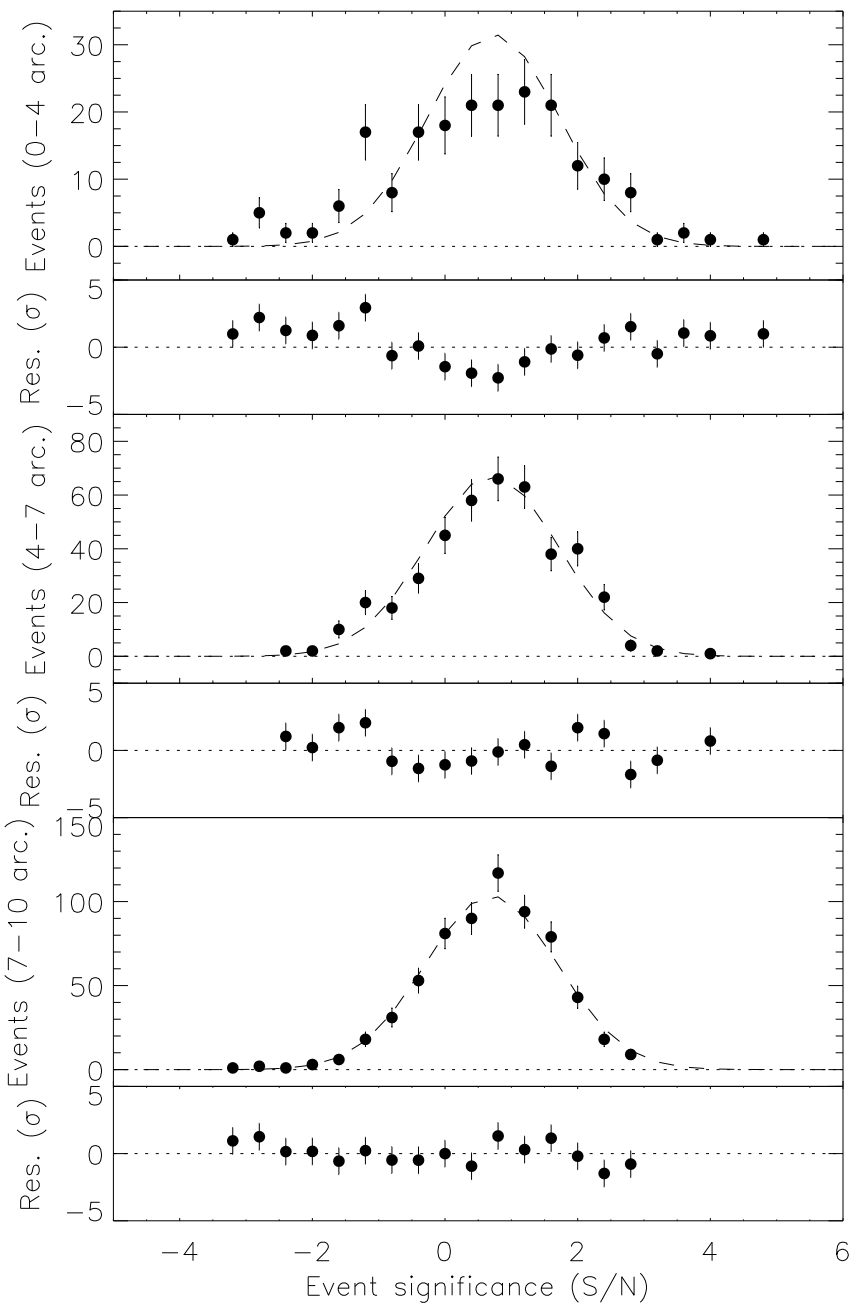
Events (0−4 arc.)
Res. (σ)
Events (4−7 arc.)
Res. (σ)
Events (7−10 arc.)
Res. (σ)
Event significance (S/N)

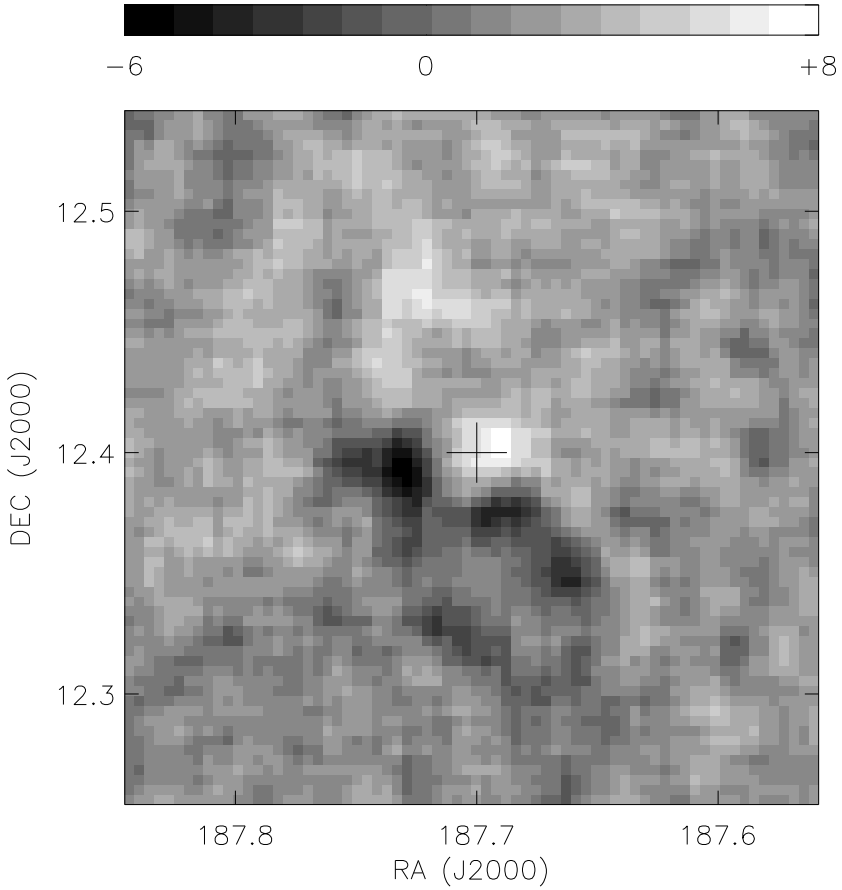
−6
0
+8
12.5
12.4
12.3
DEC (J2000)
187.8
187.7
187.6
RA (J2000)

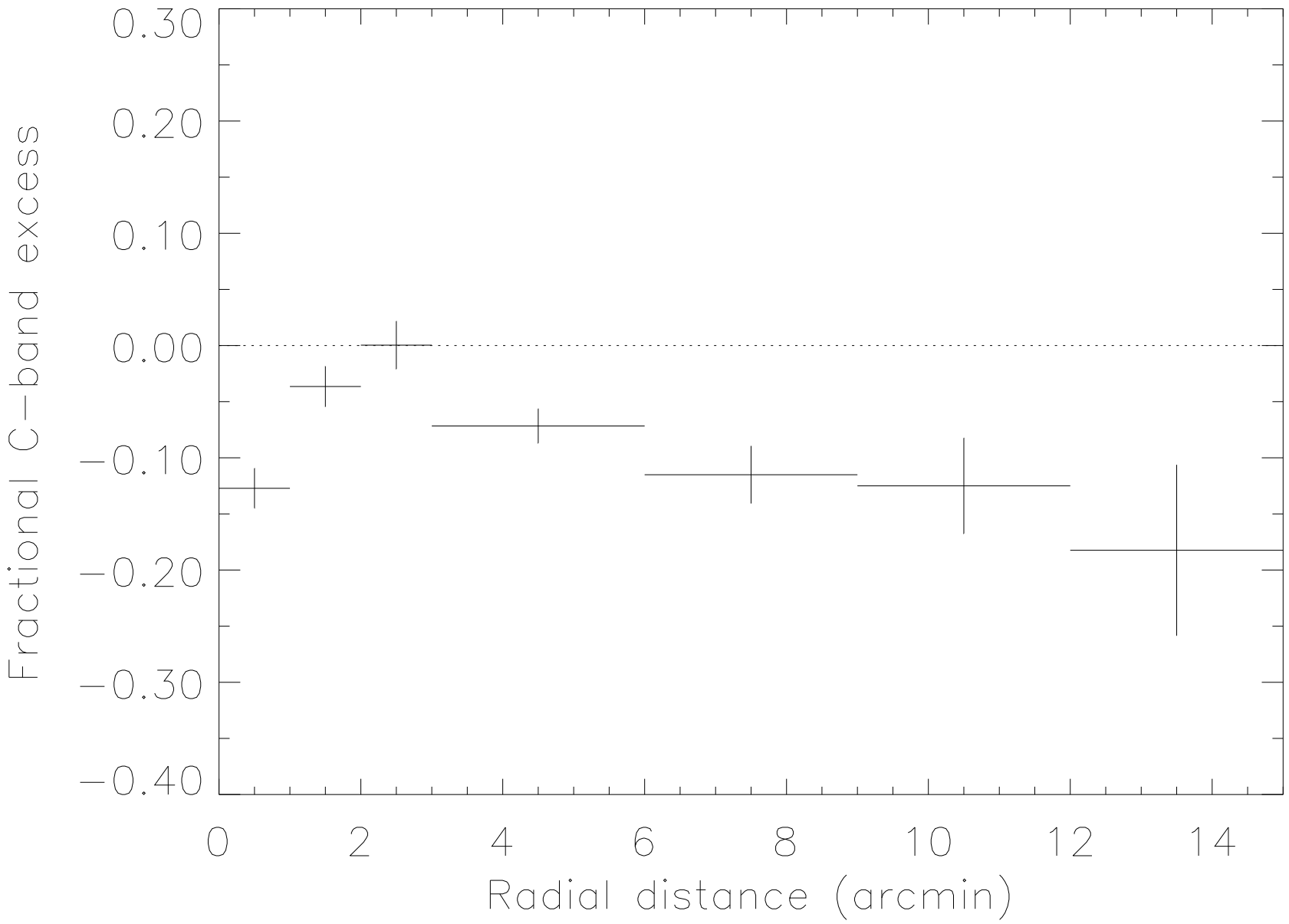
0.30
0.20
0.10
0.00
−0.10
−0.20
−0.30
−0.40
Fractional C−band excess
0
2
4
6
8
10
12
14
Radial distance (arcmin)

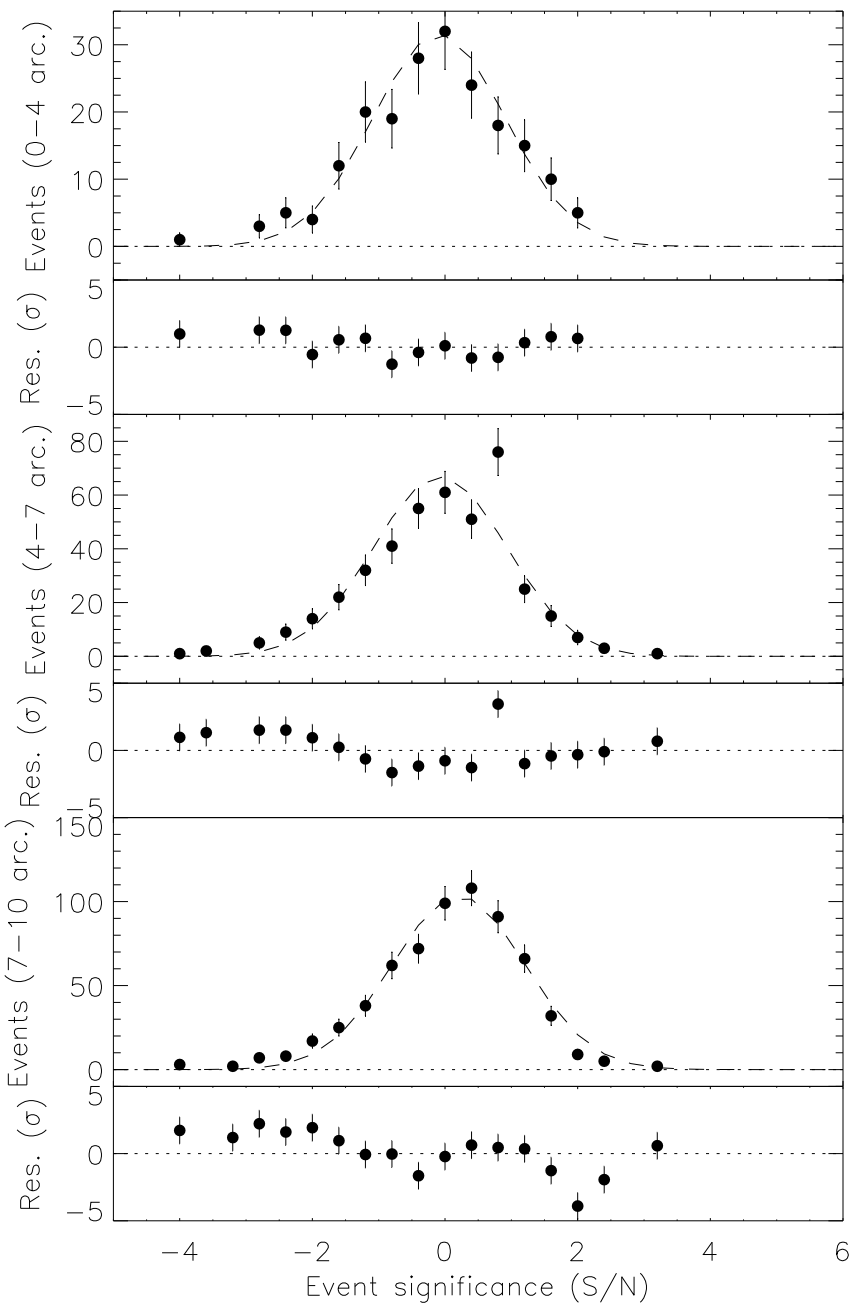
Events (0−4 arc.)
Res. (σ)
Events (4−7 arc.)
Res. (σ)
Events (7−10 arc.)
Res. (σ)
Event significance (S/N)

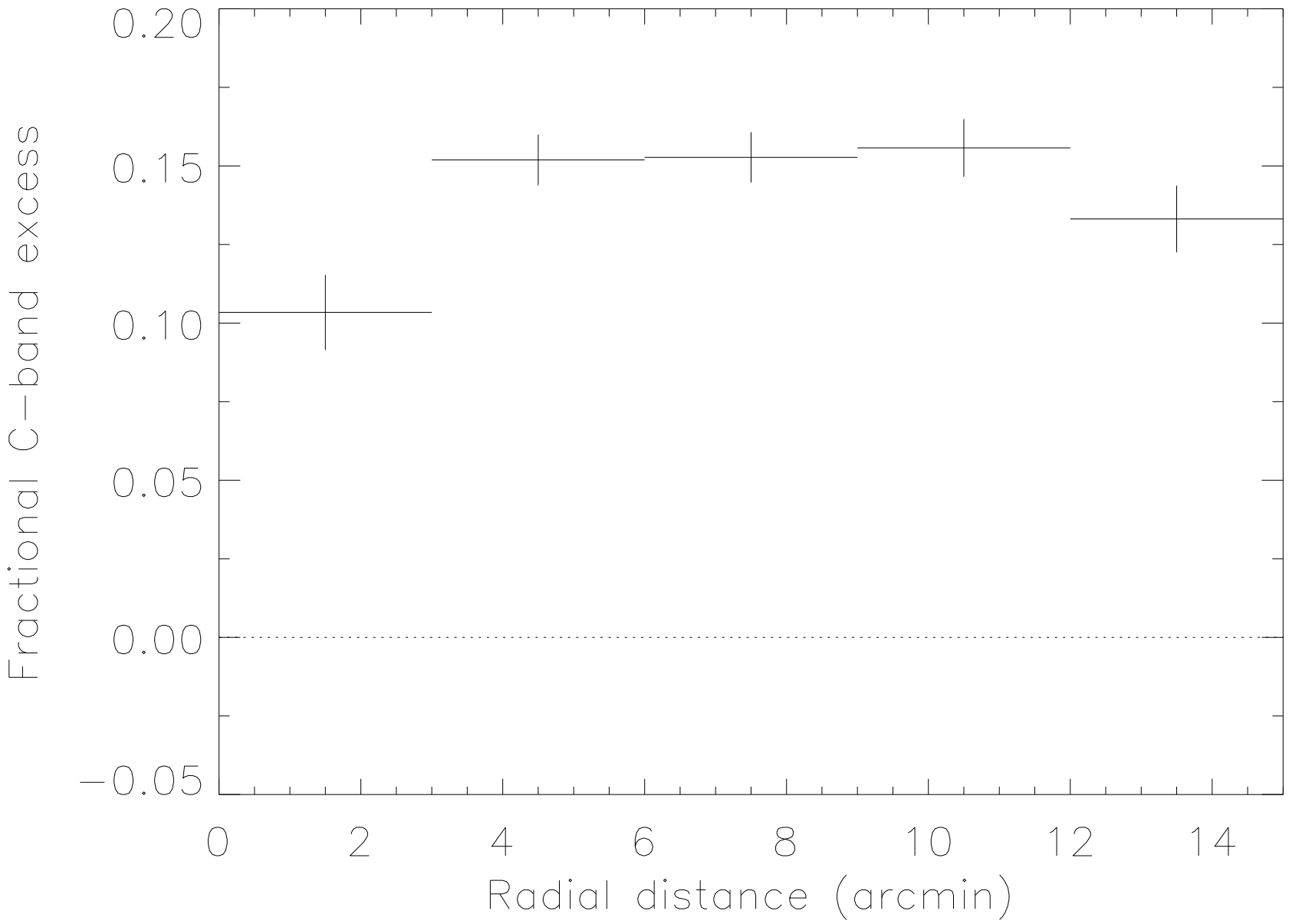
0.20
0.15
0.10
0.05
0.00
−0.05
Fractional C−band excess
0
2
4
6
8
10
12
14
Radial distance (arcmin)

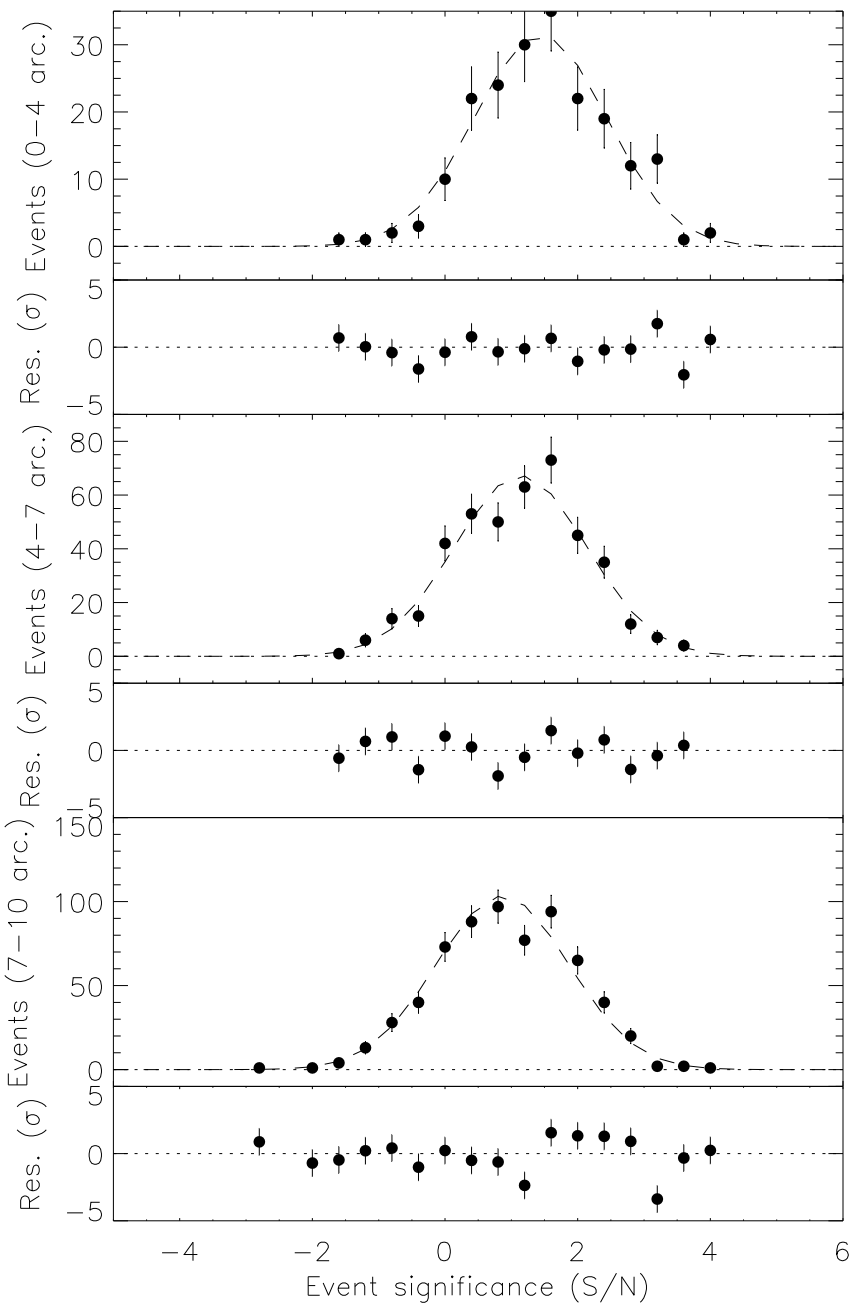
Events (0−4 arc.)
Res. (σ)
Events (4−7 arc.)
Res. (σ)
Events (7−10 arc.)
Res. (σ)
Event significance (S/N)